Available online at www.sciencedirect.com
ScienceDirect
Journal of Power Sources 174 (2007) 711–715
JOURNAL OF POWER SOURCES
www.elsevier.com/locate/jpowsour

Short communication

Magnetism and lithium diffusion in Li_xCoO_2 by a muon-spin rotation and relaxation (μ^+SR) technique

Kazuhiko Mukai [a,*], Jun Sugiyama [a], Yutaka Ikedo [a], Hiroshi Nozaki [a], Koichiro Shimomura [b], Kusuo Nishiyama [b], Kingo Ariyoshi [c], Tsutomu Ohzuku [c]

[a] *Toyota Central Research and Development Laboratories, Inc., Nagakute, Aichi 480-1192, Japan*
[b] *High Energy Accelerator Research Organization (KEK), Tsukuba, Ibaraki 305-0801, Japan*
[c] *Department of Applied Chemistry, Graduate School of Engineering, Osaka City University (OCU), Osaka 558-8585, Japan*

Available online 27 June 2007

Abstract

Microscopic magnetism of the electrochemically Li-deintercaleted Li_xCoO_2 powders has been investigated by muon-spin rotation and relaxation (μ^+SR) spectroscopy in the temperature (T) range between 10 and 300 K. Weak transverse-field μ^+SR measurements indicate that localized moments appear in $LiCoO_2$ below 60 K, while both $Li_{0.53}CoO_2$ and $Li_{0.04}CoO_2$ are paramagnetic even at 10 K. Zero-field μ^+SR measurements for the samples with $x = 0.53$ and 0.04 show that the field distribution width (Δ) due to randomly oriented nuclear magnetic moments of ^{7}Li and ^{59}Co decreases monotonically with increasing T up to 250 K, and then it decreases steeper (increasing slope ($d\Delta/dT$)) above 250 K. Because the muon hopping rate (ν) is almost T independent for $Li_{0.53}CoO_2$ below 300 K, the decrease in Δ suggests that the time scale of Li^+ diffusion in Li_xCoO_2 is within a microsecond scale.

Keywords: Lithium-ion battery; $LiCoO_2$; Muon-spin rotation and relaxation (μ^+SR); Magnetism; Diffusion

1. Introduction

Lithium cobalt dioxide, $LiCoO_2$ has been extensively studied as a positive electrode material for Li-ion batteries over the past decade. According to ^{7}Li NMR [1] and magnetic susceptibility (χ) measurements [2], the electronic configuration of Co^{3+} in $LiCoO_2$ is in its low-spin state (t_{2g}^6), suggesting the absence of magnetic transitions at low temperatures (T). Sugiyama et al. [3], however, reported the appearance of localized moments below 65 K and long-range antiferromagnetic (AF) order below 30 K by muon-spin rotation and relaxation (μ^+SR) experiments, which is very sensitive to the local magnetic order. This suggests that either partial spin state transition ($t_{2g}^6 \rightarrow t_{2g}^5 e_g^1$) or a charge seperation ($2Co^{3+} \rightarrow Co^{2+} + Co^{4+}$) occurs below 65 K for $LiCoO_2$. However, such AF order was not observed for the Li_xCoO_2 samples with $x = 0.95$ and 0.70 [3]. Further Li^+ deintercalation induces structural phase transitions from the rhombohedral ($R\bar{3}m$) to the monoclinic ($C2/m$) phase at $0.5 \leq x \leq 0.55$ [4], and then O3 to O1 at $x \leq 0.25$ [5,6]. This leads to the question on the correspondence between magnetism and crystal structures particularly for the Li_xCoO_2 with $x \leq 0.55$.

In order to examine the relation between magnetism and structure in Li_xCoO_2, μ^+SR experiments for the samples with $x = 0.53$ and 0.04 are carried out because only μ^+SR detects the magnetic transition of Li_xCoO_2 with $x \geq 0.7$. Again, μ^+SR is a powerful technique to detect both static and dynamic internal magnetic fields of nuclear and electronic origin, and it gives essential information for understanding magnetic properties on a microscopic scale [7]. Recently, it is found that μ^+SR provides useful information on Li^+ mobility by detecting change in nuclear dipole fields as was reported for $LiMn_2O_4$ and related materials [8,9]. In this paper, we report μ^+SR results on microscopic magnetism for Li_xCoO_2 and discuss the relation between magnetism and structure together with Li^+ diffusion.

2. Experimental

A stoichiometric $LiCoO_2$ was prepared from $LiOH{\cdot}H_2O$ and $CoCO_3$ as described previously [4]. Starting materials were well

* Corresponding author.
E-mail address: e1089@mosk.tytlabs.co.jp (K. Mukai).

0378-7753/$ – see front matter © 2007 Elsevier B.V. All rights reserved.
doi:10.1016/j.jpowsour.2007.06.111

mixed and pressed into pellets (23 mm diameter and ∼5 mm thickness). The pellets were heated at 900 °C for 12 h in air. The sample was characterized by powder X-ray diffraction (XRD) and electrochemical measurements.

The Li_xCoO_2 samples for μ^+SR experiments were prepared by an electrochemical reaction in non-aqueous Li cells. In order to avoid μ^+SR signals from conducting carbon and binder, the electrodes were made of only the $LiCoO_2$ powder (a disc with 23 mm diameter and ∼0.3 mm thickness). The electrolyte used was 1 M $LiPF_6$ dissolved in ethylene carbonate (EC)/diethyl carbonate (DEC) (1/1, v/v) solution.

μ^+SR requires low-energy muons, so that they stop in samples within 100–200 mg cm^{-2} depth. High intensity beams are produced by high-energy (>500 MeV) proton accelerators. The muon beams are distinguishable by their time structure. Paul Scherrer Institut (PSI) in Switzerland and Tri-University Meson Facility (TRIUMF) in Canada are both *continuous wave* facilities, while high energy accelerator research organization (KEK) in Japan and Rutherford Appleton Laboratory (RAL) in the UK are sources of *pulsed* muon beam. The *continuous wave* facilities are suitable for the detection of larger magnetic fields and fast relaxing signals. The *pulsed* muon beam facilities are ideal for studying relatively slow relaxation, such as muon diffusion. In this study, we focused on the both local magnetism and muon diffusion, so that we have performed the μ^+SR experiments in the surface muon channel (π_A port) in KEK.

Each Li-deintercalated sample electrochemically prepared was packed in a sealed aluminum sample cell in a He-filled glove-box, and then placed on the silver sample holder in a cryostat. μ^+SR spectra were measured in a zero-field (ZF-), longitudinal-field (LF-) and weak transverse-field (wTF-) mode in the T range between 10 and 300 K. The orientations of external magnetic field are parallel for LF-, and perpendicular for wTF-, respectively, to the initial direction of muon-spin polarization.

After the μ^+SR experiments, the Li-cells were re-fabricated using the Li-deintercalated samples and their open circuit voltages (OCV) were measured in order to examine whether or not one-to-one correspondence μ^+SR signal and structure holds via electrochemical data. Magnetic susceptibility χ was measured using a superconducting quantum interference device (SQUID) magnetometer (MPMS, Quantum Design) in the T range between 5 and 400 K under magnetic field $H = 10$ kOe. Other sets of experimental conditions are given in Section 3.

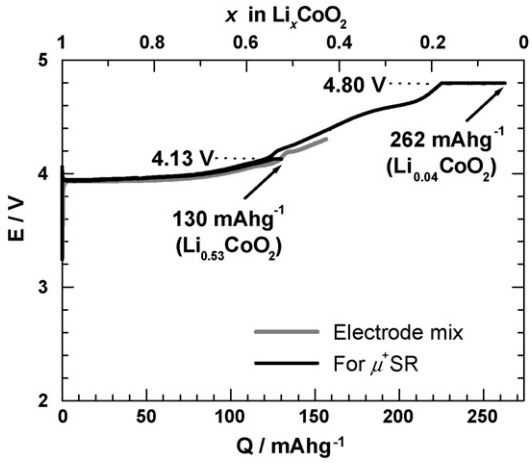

Fig. 1. Charge curves of Li/$LiCoO_2$ cells operated at a rate of 0.72 mA cm^{-2} at 25 °C. At 4.13 (or 4.8 V), the cell was potentiostatically charged totally for 3 days. The charge curve of the cell using the electrode mix, which consists of 88 wt.% $LiCoO_2$, 6 wt.% conductive carbon and 6 wt.% binder, is also shown for comparison. The Li composition was calculated from Q and theoretical capacity (274 mAh g^{-1}) based on one-electron transfer per formula weight of $LiCoO_2$.

3. Results and discussion

3.1. Characterization of Li_xCoO_2

$LiCoO_2$ was identified as a layered structure ($a = 2.814$ Å, $c = 14.049$ Å) with a space group symmetry of $R\bar{3}m$, in which cobalt- and lithium-ions were, respectively, located at the octahedral 3a and 3b sites in a cubic close-packed oxygen array. Fig. 1 shows the charging curves $E(Q)$ of Li/$LiCoO_2$ cells operated at a rate of 0.72 mA cm^{-2} (ca. 6 mA g^{-1}) at 25 °C. The values of x for the present Li_xCoO_2 samples with $x = 0.53$ and 0.04 were calculated from the theoretical capacity of 274 mAh g^{-1} assuming one-electron transfer per formula weight of $LiCoO_2$ and 100% of coulombic efficiency. Electrochemical charge was carried out up to 4.13 or 4.8 V at which the cell was potentiostatically charged totally for 3 days. The operating voltage (E) for 0 to 70 mAh g^{-1} is almost constant, and then the $E(Q)$ curve monotonically increases in voltage as a function of Q. Two minor changes in the slope of the $E(Q)$ curve are observed around 125 mAh g^{-1} and 200 mA g^{-1}. The former corresponds to the phase transition from the $R\bar{3}m$ to the $C2/m$ phase [4], and the latter shows the change in oxygen packing from the O3 to the O1 [5,6]. These $E(Q)$ curves for the electrodes prepared without the addition of conducting carbon and binder are almost the same to those of usual electrode mix as seen in Fig. 1. After the whole

Table 1
The Li/Co ratio of the Li_xCoO_2 samples and open circuit voltages (OCV) of the Li/Li_xCoO_2 cells before and after the μ^+SR and χ measurements

Li/Co (EC)	OCV (μ^+SR)		OCV (χ) (∼150 h[a])	Li/Co (ICP-AES) (∼180 h[a])
	Before (0 h[a])	After (∼12 h[a])		
0.53	4.13 V	4.11 V	4.08 V	0.50
0.04	4.43 V	4.38 V	4.41 V	0.12

ICP-AES analysis was carried out after the whole measurements: that is, ∼1 week later after the initial electrochemical charge (EC). The Li/Co ratio of the $LiCoO_2$ sample is 1.02.

[a] Time after the charge.

μ^+SR and χ measurements, the composition of the samples was determined by an induction coupled plasma-atomic emission spectral (ICP-AES) analysis. The samples were washed with acetone and dried. The results are summarized in Table 1. The Li/Co ratio calculated by an electrochemical measurement is usually different from that by an ICP-AES analysis mainly due to the decomposition of the electrolyte especially at higher voltage than 4.5 V. The Li/Co ratios for the present samples are thus estimated to be within $0.50 \leq x \leq 0.53$ and $0.04 \leq x \leq 0.12$ in Li_xCoO_2. Although the structural analysis of these samples was not performed, the $E(Q)$ curves and the value of OCV support that the sample with $0.50 \leq x \leq 0.53$ is the monoclinic phase [4] and with the $0.04 \leq x \leq 0.12$ the O1 phase [5,6]. In this paper, the Li/Co ratios calculated from electrochemical data were used.

3.2. Micro- and macroscopic magnetism of Li_xCoO_2

In order to examine the existence/absence of magnetic phase transitions and/or volume fraction of magnetic phases, wTF-μ^+SR spectra were measured in magnetic field of ~20 Oe for the Li_xCoO_2 samples with $x = 1$, 0.53, 0.04. The T dependence of wTF-μ^+SR time spectra are shown in Fig. 2 for the $x = 0.53$ sample at 100 and 10 K. Open circles indicate the given experimental data and solid lines the fitting result using the function of

$$A_0 P_{TF}(t) = A_{TF} \exp(-(\lambda t)^{\beta}) \cos(\omega_\mu t + \varphi) \quad (1)$$

where A_0 is the empirical initial muon asymmetry, $P_{TF}(t)$ the muon-spin depolarization function, ω_μ the muon Larmor frequency in the applied field, φ the initial phase of the precession, A_{TF} and λ are, respectively, the asymmetry and the exponential relaxation rate of the oscillation caused by the external wTF and β is the power of the exponential relaxation. The asymmetry indicates muon-spin depolarization by the local magnetic fields in the sample. If the sample has weak internal fields, such as due to paramagnetism or nuclear magnetism, A_{TF} is independent of T. Conversely, ferromagnetic or antiferromagnetic order generates in the sample, A_{TF} decreases in proportion to the volume of the magnetic phases. Therefore, $A_{TF}(T)$ curve is very useful to know the magnetic transition and the volume fraction of the magnetic phase.

Fig. 3 shows the T dependence of A_{TF} for the samples with $x = 1$, 0.53 and 0.04. The normalized A_{TF} (N_{ATF}) is defined by $[A_{TF}(100\,K) - A_{TF}(T)]/A_{TF}(100\,K)$. When T decreases from 100 K, N_{ATF} for the $x = 1$ sample is almost constant (~1) down to 60 K, and then drops with further decreasing T. This clearly indicates that the sample is approximately 100% paramagnetic above 60 K, and enters into a magnetic phase below 60 K. The volume fraction of the magnetic phase is ca. 13% at 10 K, as reported previously [3]. The magnetic Co^{3+} ($S = 1$) in the CoO_5 square-based pyramid was observed in non-stoichiometric compounds, such as $Li_{1.08}CoO_2$ [10]. However, the existence of the change in voltage around $x = 1/2$ in the $E(Q)$ curve in Fig. 1 suggests that the present sample is the stoichiometric $LiCoO_2$, because the change around $x = 1/2$ is a characteristic of stoichiometric $LiCoO_2$ [4]. Since the low-spin Co^{3+} (t_{2g}^6) ions are non-magnetic, the origin of this magnetism is probably due to a partial spin state transition ($t_{2g}^6 \rightarrow t_{2g}^5 e_g^1$) [11] or a charge seperation reaction ($2Co^{3+} \rightarrow Co^{2+} + Co^{4+}$) as already reported [3]. For the Li-deintercalated samples, N_{ATF} is almost constant over an entire T range for the $x = 0.53$ and 0.04 samples, indicating absence of magnetic order even at 10 K.

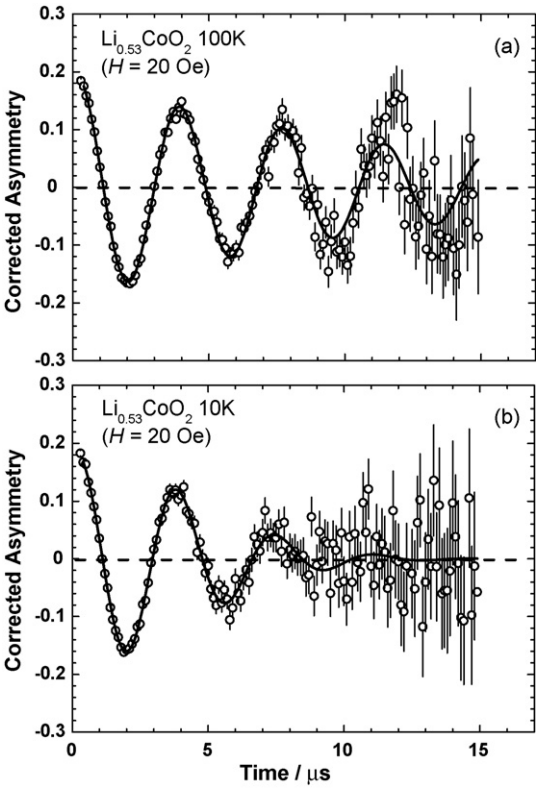

Fig. 2. wTF-μ^+SR time spectra for the Li_xCoO_2 sample with $x = 0.53$ at: (a) 100 K and (b) 10 K. Open circles and solid lines indicate the experimental data and the fitting result using Eq. (1), respectively. The orientation of the external magnetic field (transverse-field) is perpendicular to the initial direction of muon-spin polarization. A clear oscillation due to the external field is observed both 100 and 10 K. Although the bottom spectrum shows a larger relaxation than that of top, the initial amplitude does not change with T. This indicates $Li_{0.53}CoO_2$ is paramagnetic at 10 K.

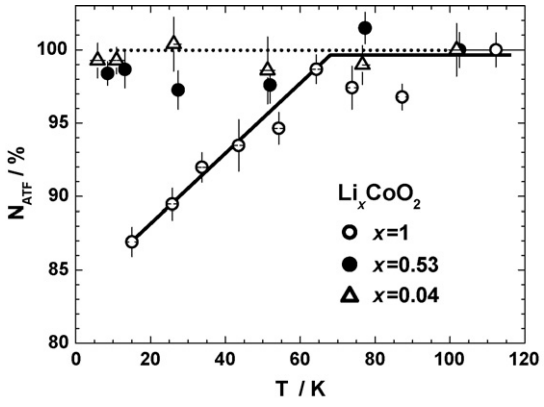

Fig. 3. Temperature dependence of the normalized asymmetry ($N_{A_{TF}}$) for the samples with $x = 1$, 0.53 and 0.04. Data were obtained by fitting the wTF-μ^+SR spectra using Eq. (1). N_{ATF} is defined as $[A_{TF}(100\,K) - A_{TF}(T)]/A_{TF}(100\,K)$.

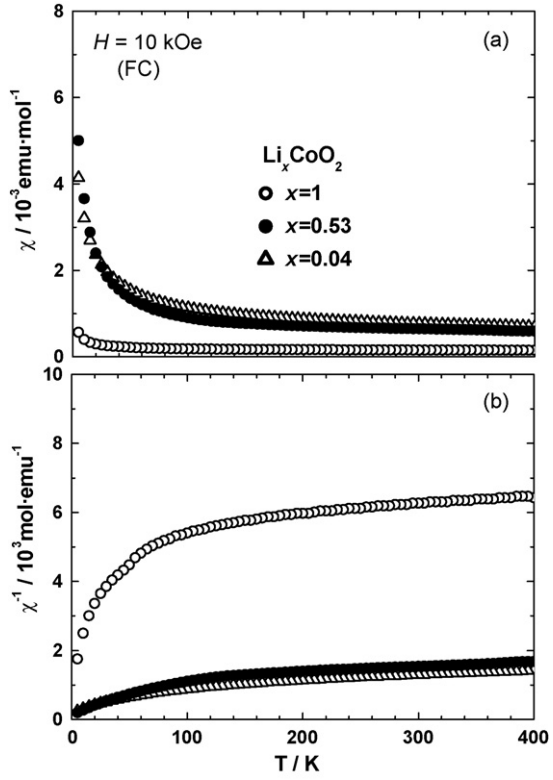

Fig. 4. (a) χ and (b) χ^{-1} as a function of temperature for the Li_xCoO_2 samples with $x = 0$, 0.53 and 0.04, measured in field-cooling (FC) mode with $H = 10$ kOe.

Fig. 4 shows (a) the $\chi(T)$ and (b) $\chi^{-1}(T)$ curves for the three samples. The $\chi(T)$ curve was measured in field-cooling (FC) mode with $H = 10$ kOe. After the μ^+SR experiment, the OCV of the cell were 4.11 V for the $x = 0.53$ sample and 4.38 V for $x = 0.04$, respectively. These values are 0.02–0.05 V lower than those measured before the μ^+SR experiment. The $\chi(T)$ curve for the $x = 1$ sample shows paramagnetic behavior down to 5 K. On the other hand, the $\chi(T)$ curves for both $x = 0.53$ and 0.04 samples are almost T independent down to 100 K, indicating a Pauli paramagnetic behavior. This is consistent with the insulator to metal transition induced by the decrease in Li at $x = 0.95$ [12]. The magnetic transition around 170 K for the $x = 0.95$, 0.70 [3] or 0.5 [2] samples, is not observed in the present two samples. As seen in Figs. 3 and 4, $x = 0.53$ and 0.04 samples are paramagnetic even at 10 K, confirming the lack of magnetic order both macro- and microscopically. This also supports that there is no direct correlation between phase transition and magnetism for the $x \leq 0.55$ samples.

Fig. 5 shows the T dependence of ZF-μ^+SR time spectra for the $x = 0.53$ sample at 300, 250, 200 and 10 K. Solid lines represent the fitting results obtained using the dynamic Kubo-Toyabe function $G^{DGKT}(t, \Delta, \nu)$ due to randomly oriented nuclear magnetic moments [13];

$$A_0 P(t) = A_{KT} G^{DGKT}(t, \Delta, \nu) + A_{BG} \quad (2)$$

where A_{KT} and A_{BG} are, respectively, the asymmetries of dynamic Kubo-Toyabe component and background signals mainly from the silver sample cell, Δ the static width of the

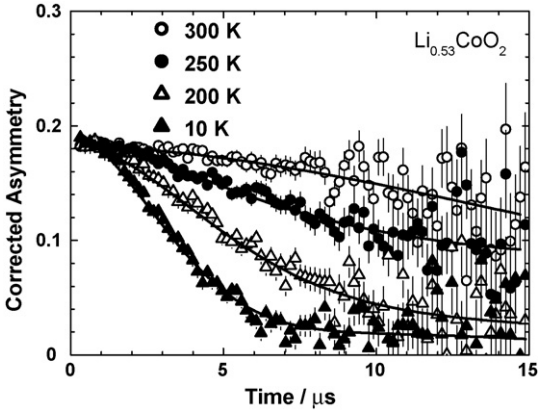

Fig. 5. ZF-μ^+SR time spectra for the Li_xCoO_2 sample with $x = 0.53$ at 300, 250, 200 and 10 K. Solid lines represent the results of fitting using Eq. (2).

local fields at the disordered sites and ν is the muon hopping or field fluctuation rate. When $\nu = 0$, $G^{DGKT}(t, \Delta, \nu)$ is the static Gaussian Kubo-Toyabe function $G^{KT}(t, \Delta)$ given by

$$G^{KT}(t, \Delta) = \frac{1}{3} + \frac{2}{3}(1 - \Delta^2 t^2)\exp\left(\frac{-\Delta^2 t^2}{2}\right) \quad (3)$$

As seen in Fig. 5, neither fast relaxation nor rotation is observed in these spectra, indicating that muon-spin is depolarized mainly by nuclear moments of ^{7}Li (4.20 μ_N) and ^{59}Co (5.25 μ_N).

Fig. 6 shows the T dependence of (a) Δ and (b) ν for the $x = 1$, 0.53 and 0.04 samples. Although Δ and ν for $LiCoO_2$ are

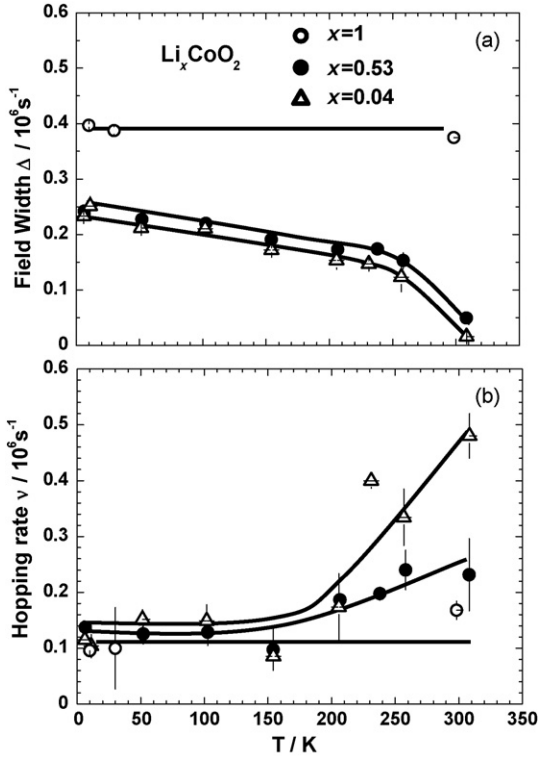

Fig. 6. Temperature dependence of (a) field distribution width Δ and (b) muon hopping rate ν for the Li_xCoO_2 samples with $x = 1$, 0.53 and 0.04. Both Δ and ν were estimated by fitting the ZF- and LF-μ^+SR time spectra using Eq. (2).

virtually independent of T, Δ for the $x<1$ samples decreases gradually with increasing T up to 250 K, and then decreases more rapidly. This may be a similar phenomenon to motional narrowing of the ^{7}Li NMR line shape at ∼400 K [14]. Considering the measurement accuracy of ν, the $\nu(T)$ curve for the $x=0.53$ sample is almost T independent even at $T>200$ K. The rapid decrease in Δ above 250 K would therefore correlate with the change in Li^+ diffusion as already reported for $LiMn_2O_4$ and related materials [8,9]. On the contrary, ν increases rapidly above 250 K for the $x=0.04$ sample when T increases. This means that muon diffusion in the lattice begins above 250 K. Since ν is almost T independent for both $Li[Li_{0.04}Mn_{1.96}]O_4$ and $Li_{0.2}[Li_{0.04}Mn_{1.96}]O_4$ [8], the difference in the $\nu(T)$ curves between $Li_{0.04}CoO_2$ and $Li_{0.2}[Li_{0.04}Mn_{1.96}]O_4$ is probably due to the difference in "ion channel", i.e., two-dimensional channel in $LiCoO_2$ versus three-dimensional channel consisting of one-dimensional tunnels in $LiMn_2O_4$.

As stated above, μ^+SR is an effective tool to characterize lithium insertion materials in terms of both magnetic behavior and Li^+-ions dynamics. In this paper, we have reported the results on μ^+SR experiments for the Li_xCoO_2 samples with $x=0.53$ and 0.04. In order to determine the full phase diagram of Li_xCoO_2, further μ^+SR experiments are necessary in particular for the $0.5\leq x\leq 0.7$ samples. Such experiments are still in progress in our research group.

Acknowledgements

We wish to thank Mr. S. Kohno of OCU for preparing sample of $LiCoO_2$ and Mr. Y. Kondo of Toyota Central R&D Labs., Inc. for measuring ICP-AES analysis. We also appreciate Prof. J.H. Brewer of University of British Columbia and Prof. E.J. Ansaldo of TRIUMF for fruitful discussions.

References

[1] M. Ménétrier, A. Rougier, C. Delmas, Solid State Commun. 90 (1994) 439–442.
[2] S. Kikkawa, S. Miyazaki, M. Koizumi, J. Solid State Chem. 62 (1986) 35–39.
[3] J. Sugiyama, H. Nozaki, J.H. Brewer, E.J. Ansaldo, G.D. Morris, C. Delmas, Phys. Rev. B 72 (2005) 144424.
[4] T. Ohzuku, A. Ueda, J. Electrochem. Soc. 141 (1994) 2972–2977.
[5] G.G. Amatucci, J.M. Tarascon, L.C. Klein, J. Electrochem. Soc. 143 (1996) 1114–1123.
[6] L. Liu, L. Chen, X. Huang, X.-Q. Yang, W.-S. Yoon, H.S. Lee, J. McBreen, J. Electrochem. Soc. 151 (2004) A1344–A1351.
[7] J.H. Brewer, Encyclopaedia Appl. Phys. 11 (1994) 23–53 (and references cited therein).
[8] C.T. Kaiser, V.W.J. Verhoeven, P.C.M. Gubbens, F.M. Mulder, I. de Schepper, A. Yaouanc, P. Dalmas de Réotier, S.P. Cottrell, E.M. Kelder, J. Schoonman, Phys. Rev. B 62 (2000) R9236–R9239.
[9] M.J. Ariza, D.J. Jones, J. Roziere, J.S. Lord, D. Ravot, J. Phys. Chem. B 107 (2003) 6003–6011.
[10] S. Levasseur, M. Ménétrier, Y. Shao-Horn, L. Gautier, A. Audemer, G. Demazeau, A. Largetew, C. Delmas, Chem. Mater. 15 (2003) 348–354.
[11] M. Mikami, M. Yoshimura, Y. Mori, T. Sasaki, R. Funabashi, M. Shikano, Jpn. J. Appl. Phys. 42 (2003) 7383–7386.
[12] M. Ménétrier, I. Saadoune, S. Levasseur, C. Delmas, J. Mater. Chem. 9 (1999) 1135–1140.
[13] R.S. Hayano, Y.J. Uemura, J. Imazato, N. Nishida, T. Yamazaki, R. Kubo, Phys. Rev. B 20 (1979) 850–859.
[14] K. Nakamura, H. Ohno, K. Okamura, Y. Michihiro, I. Nakabayashi, T. Kanashiro, Solid State Ionics 135 (2000) 143–147.